

Magnetic Optical Bearing (MOB) Design for Mirror Wavelength Scans in a Spaceborne Interferometer

Lawrence S. Schwartz

Spacecraft Bus Electronics, Hughes Space and Communications Company
Loc. SC, Bldg. S21, MS H350, PO Box 92919, Los Angeles, CA 90009, USA
tel: 310-335-6511; fax 310-364-9792; e-mail: Lawrence_S_Schwartz_at_6-master@ccgate.hac.com

Dr. David L. Trumper

Department of Mechanical Engineering, Massachusetts Institute of Technology
Rm. 35-016, 77 Massachusetts Avenue, Cambridge, MA 02139, USA
tel: 617-253-3481; fax 617-253-7549; e-mail: trumper@mit.edu

Abstract: NASA maintains the Geosynchronous Operational Environmental Satellite (GOES) fleet for severe weather observation and anomalous atmospheric behavior, such as the greenhouse effect. A critical instrument flown on these satellites is the Fourier Transform Infrared (FTIR) interferometer used for atmospheric element detection. Traditionally, the scanning element of this device has relied on mechanical designs such as flexures to yield long term, reliable, and accurate scanning motion and control. Although flight tested, flexure designs are subject to wear, single-point failures, and do not usually allow corrective active control in degrees-of-freedom other than in the primary axis of motion.

Magnetic bearings designed for spaceborne interferometry can compensate for these deficiencies. However, previous designs been large, heavy and inefficient. This paper discusses a novel magnetic bearing configuration which alleviates these problems by using magnetic hybrid actuators. Here, three identical two degree-of-freedom magnetic hybrid actuators comprise a six degree-of-freedom actively controlled scanning magnetic optical bearing. The design of this overall system is developed in the paper. Furthermore, a prototype of one of the three identical actuators is designed, built and tested with the results discussed. Although presented in the context of optical devices, this magnetic bearing may also be possibly used in such devices as coordinate measuring machines, linear axis control, lithographic steppers, and other precision control devices.

1 Introduction

In the design of this system, two areas of research provide the focus for the effort. The first, in a general sense, is that of general spaceborne FTIR mechanical design, focusing on the scanning mirror design to meet optical and satellite conditions. The second, in a more technical sense, is magnetic bearing technology, which is at the heart of the Magnetic Optical Bearing (MOB) design. The former field helps one to understand the broad ideas and design point requirements. The latter field provides the vehicle in which one can implement a design.

At the heart of the FTIR interferometer is the scanning mirror. Indeed "the success of rapid scanning interferometry depends principally on the engineering of the interferometer and the drive system." [1] The bearing and drive requirements on the scanning mirror are challenging. The scanning mirror must keep a constant angle of orientation with respect to the optical axis. There are several common methods of maintaining this angle. Cube corner retro-reflectors inherently compensate a scanning drive system that is incapable of preventing tilt motion of the scanning mirror. So called "cat's eye" interferometers also decrease system sensitivity to such undesirable disturbances. The first method however requires additional reflection surfaces, and the second method is rather expensive. Other, more mechanical adaptations include the "porch-swing" design (a parallelogram method) which insures a nearly constant angle with respect to the optical axis and which usually employs flexure pivots. It is a popular design that is used in the Nimbus, Voyager, and Mariner spacecraft. It is a dependable design, but inherently suffers because of its mechanical nature. Another alternative design, is the "rocking wishbone" configuration [1]. This design is a combination of a pendulum and a corner cube. However, the design here too suffers from typical mechanical drawbacks, as well as its tendency to amplify errors. Finally, the occasional use of air bearings for these scanning mirrors can be found. Combined with a linear motor, an air bearing seems like an ideal solution. However, in practice, they have been often inadequate. They have a lower load-supporting capability, need a variety of extraneous support equipment, and either have a lower stiffness, or exhibit instability at a higher one. Besides, a space application such as a satellite can hardly afford an air system. Magnetic bearings are another way to provide non-contact bearing capability, and are useful in environments such as space where an air bearing cannot venture.

In order to develop a unique suspension system, one which is tailored for the motion requirements of scanning mirror, a new and creative magnetic circuit design is required. Two fields of electromagnetic theory will be introduced in the context of the MOB design. The first, electromagnetics (EM), deals with the types of suspension forces normally associated with magnetic bearing

technology. The second, electrostatics (ES), focuses on the types of driving forces associated with voice coils and speakers. These two forces can be packaged in a complementary fashion so that a single actuator harnesses both of these capabilities.

Besides the mechanical advantages offered by non-contact nature of magnetic bearings, one other design asset is worthy of mentioning, and that is the complete, six degree-of-freedom active control found on the MOB scanning mirror. More often than not, the scanning axis is the only actively actuated degree of freedom. If alignment errors arise from the mirror (or anywhere else in the system for that matter), they often need correction from a commandable pointing mirror. In the MOB configuration, with all degrees-of-freedom controlled, small corrections in the other axes can be obtained without the use of these other mirrors. Final related advances are in disturbance rejection of unwanted vibrations and increased bandwidth with the lack of structural resonances.

Rather than relying purely on hand calculations and computer simulations alone for this project development, a decision was made to try to implement a prototype actuator for the design. The MOB configuration consists of three two degree-of-freedom actuators. In order to limit the scope of this project, the design and development of only one of these actuators was researched and implemented to prove the magnetic circuit design as viable.

Given the variety of motivations that initiated this project development, the objectives for the research were straightforward. The first objective was to design on paper a full six degree-of-freedom magnetically suspended scanning mirror. The second was to design, build, and test a prototype actuator for such a scanning mirror: a concept verification of sorts. By these objectives, the feasibility of a new magnet scanning mirror will be proven herein.

2 System Design

In order to design the prototype, first an understanding of the GOES specifications (the MOB design platform) is in order. The interferometer required for the GOES project has a variety of optically specified design points. These are summarized in table 1 below.

Table 1: Satellite requirements. (mod)

Scan speed	2.13 cm/sec
Turnaround time	25 msec
Acceleration	1.7 m/s^2 (0.2G)
Scan extent	$\pm 0.5 \text{ cm}$
Power dissipated	$\leq 0.5 \text{ Watts}$
Mass	$\leq 1 \text{ kg}$ (pref)
Velocity error	0.02 cm/sec
Life Expectancy	> 5 years

There are several requirements here that are of great importance to the prototype process. For an electromagnetic or electrodynamic system, the most difficult one to design around is the power requirement. In the design process, an electrodynamic voice coil could be made to fit within this requirement, particularly since the required acceleration is

relatively small. However, the power requirements, at least over a short duration, can be exceedingly high for any electromagnetic coils. While not consuming much power over a small region (about 10% to 20% over the entire transverse travel), if the small gaps on an electromagnetic design should see a large offset, the required aligning forces can be exceedingly large (they increase as offset squared). Scan extent inherently determines the size of any voice coil used. This extent drives the design and is an order of magnitude less than that of the Japanese Magnetically-Suspended Mirror Scanning Mechanism (MAMS) [2], the only other well published magnetic bearing scanning mirror FTIR for a space based application. The lifetime requirement should be expectedly met by use of the magnet bearing. After all, one of the reasons it is chosen as to overcome problems such as friction and wear. However, the complete system including control electronics must also meet this specification. The MOB prototype attempts to match these basic motion requirements (extent, acceleration, turnaround, and velocity) as well as mass and power.

The best way to obtain an overall picture of how the fully suspended MOB system works is to understand the kinematics and dynamics of the proposed scanning mirror. Initially, by seeing the actuator layout, an understanding of which actuators control which overall degrees of freedom can be understood. In a detailed analysis of the kinematics for this specific system, an understanding of some of the parameters that drive the system design can be gained [3].

The overall motion and control requirements for the MOB system were the initial driving forces behind the design. MAMS found one way to use electromagnets and electrostatics to suspend and control a scanning mirror. The MOB design can be thought of as a new overall approach. The decisions on where to place the assorted actuators very much determine the type of actuators required as well as their specific design requirements. To start with the analysis, an overall picture of actuator placement is shown in figure 1 below.

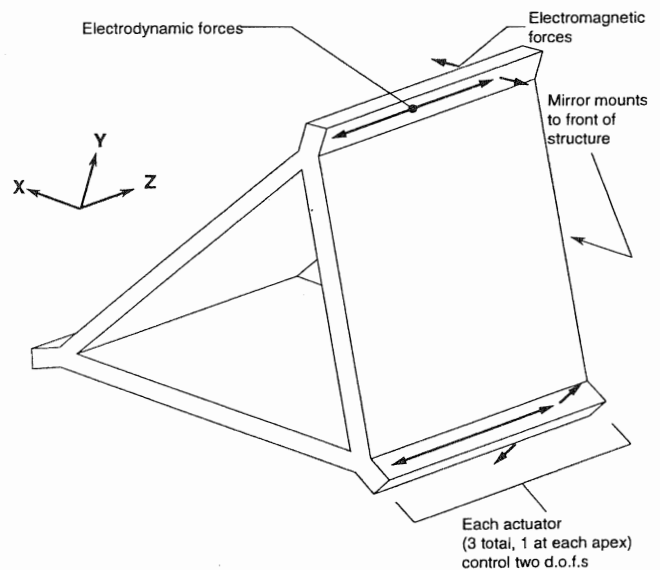


Figure 1: MOB triangular kinematics overview

The actuators are arranged in a triangular fashion, at each apex of the triangle. Each actuator can control two degrees of freedom, as indicated by the arrows. One degree-of-freedom, along the scanning direction, is controlled by means of electrodynamic forces. The other degree-of-freedom per actuator is in a direction tangential to the center of the triangle, and is controlled by means of an electromagnetic force.

A basic understanding of just how they do so can be inferred from this picture. The electrodynamic forces are all parallel to the direction of the scanning motion. The first global degree of freedom that they control with this type of motion is the scanning motion; the major motion of the body. The second and third controlled degrees-of-freedom are the tip and tilt of the mirror. Note that these are only meant to be controlled over a very small range. The electromagnetic forces handle the other degrees-of-freedom. First, the can be employed to "roll" or "spin" the body. This feature can be contrasted with the MAMS design, where only passive stabilization is used to inhibit any roll motion. The final two degrees of freedom, motion of the body in the x-y plane, can be handled by these electromagnetic forces as well. Again, these are only small translations, on the order of tens or hundreds of micrometers. This is summarized in table 2 below.

Table 2: Local to global degree-of-freedom correlation.

Control type	Degrees controlled
Electromagnetic (E-core coils)	X & Y translation Roll (about Z)
Electrodynamic (Voice coils)	Z translation (scan) Pitch (about x) Yaw (about y)

3 Magnetic Circuit

The arrangement of actuators as described in the last section is one of the novel ideas for the scanning mirror design. What will be presented now is the new magnetic circuit design proposed to make the system a reality. Figure 2 indicates the geometric parameters and the physical composition of the actuator.

The critical dimensions from for figure 2 are as follows. g defines the nominal size of the small gap, t describes the thickness of the outer leg of the E-core (note the middle leg is twice this), d is the side E-core depth into the page, h is the height of the large voice coil gap, and n is the area of the through face of the permanent magnet normalized by $d \cdot t$. Also shown is the voice coil volume V as well as the cross sectional area A of the electromagnetic coils. Other frequently used parameters include μ_0 , and M , material properties, and J , the current density in the coils.

A highly permeable core is used. A laminated iron core is specified, to maximize the allowable flux buildup in the cores as well as to reduce the effects of eddy currents, which limit the frequency response. Next is the permanent magnet, key to both parts of the circuit. Wire coils are used in two capacities, one for the electromagnetic flux generation, the other serving as a voice coil. In this drawing, only the outline of a support structure is used, since a lot of pieces must come together and be held in place. The resulting

displacements and forces will be gradually developed. Keep in mind though for now that electromagnetics will be used to exert control in and out of the page (as viewed from the left side drawing), while electrodynamics will be used to exert control left to right as seen on the page (again, as viewed from the left drawing).

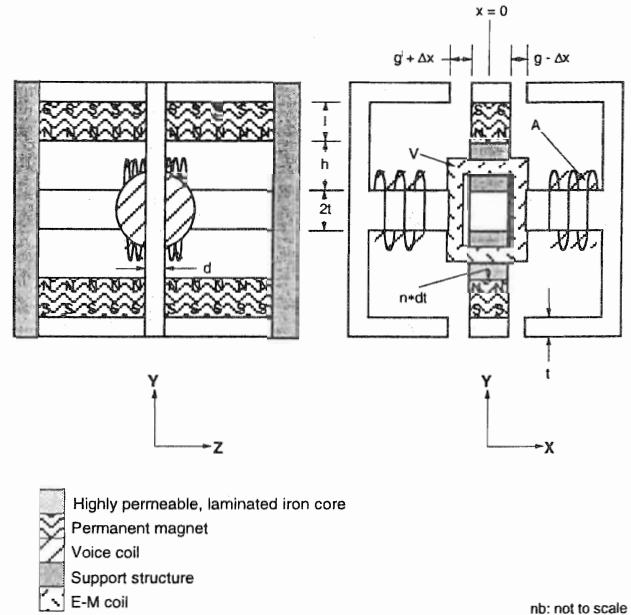


Figure 2: MOB overall design.

The permanent magnets provide a bias flux which passes through the voice coil gaps, passes down each of the upper moving cores, crosses the gaps into the upper and lower legs of the E-cores, and returns through the center leg of the E-core to the center moving core, and thereby to the back side of the permanent magnets.

Carrying out the analysis (two-dimensional and assuming that the iron has a near infinite permeability) yields the following results for the large gaps (in terms of magnetic flux density).

$$B_{Large} = \frac{\mu_0 M_0 l g}{g(h+l+ng) - n\Delta x^2} \quad (1)$$

The B-fields can be summed at the small gaps and used to find resultant electromagnetic forces.

$$B_{small(left)} = \frac{\mu_0}{2} \left[\frac{M_0 n (g - \Delta x) l}{g(h+l+ng) - n\Delta x^2} + \frac{JA}{2g} \right] \quad (2)$$

$$B_{small(right)} = \frac{\mu_0}{2} \left[\frac{M_0 n (g + \Delta x) l}{g(h+l+ng) - n\Delta x^2} - \frac{JA}{2g} \right] \quad (3)$$

Since the coil current density vector is perpendicular to the large gap B-field, the electrodynamic force is therefore

$$F_{ED} = \frac{\mu_0 M g l J V}{g(h+l+ng) - n\Delta x^2} \quad (4)$$

Plugging in for the known values of the B-fields yields the full force equation in the small gaps,

$$F_{EM(tot)} = \mu_0 dt M_0 n l \left[\frac{2 M n g l \Delta x}{[g(h+l+ng) - n \Delta x^2]^2} \right] - \mu_0 dt M_0 n l \left[\frac{A J}{g(h+l+ng) - n \Delta x^2} \right] \quad (5)$$

To meet the satellite requirements specified earlier, an intense design trade ensued, maximizing the efficiency of both sets of coils, and minimizing the system size, power, unstable pole across the small gaps, and weight. This resulted in the design point specified in table 3.

Table 3: Design point table.

Stroke	± 0.5 cm
Dissipated power	0.1 W
SiFe flux (op & max)	0.4 T, 1.3 T
Large gap flux	0.34 T
EM F/A	17 N/cm ²
ED F/V	0.3 N/cm ³
Small gap size	2 mm
Total moving weight	337 g
Perm. mag material	SmCo

Figure 3 shows a schematic what the assembled actuator and platen look like without the voice coils.

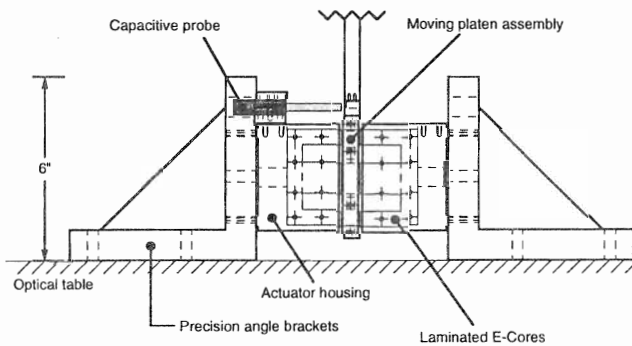


Figure 3: Overview of actuator, platen, and probe.

The setup is shown in the picture, figure 4.

4 Control System

The basic operating equations that were derived in the last section simplify very nicely and are easy to comprehend when the actuator is centered. The off-center results become more complex, particularly for the small gap forces. The off-center case is best addressed when the equations of the last

section for the forces are linearized. This is a particularly useful step for developing linear control algorithm.

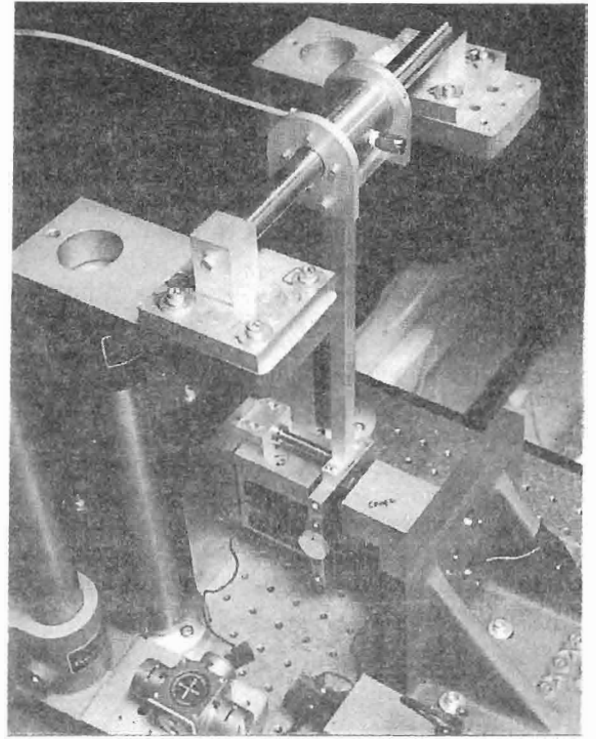


Figure 4: Top view picture of overall layout.

The electromagnetic forces, based on offset position and input current, can be re-written in state-space form, as shown in the following equations,

$$\dot{x}_1 = x_2 \quad (6)$$

$$\dot{x}_2 = \frac{c_1}{M} \left[\frac{c_2 x_1}{(c_3 - x_1^2)^2} - \frac{c_4 i}{(c_3 - x_1^2)} \right] + \frac{F_d}{M} \quad (7)$$

To arrive at this form, the offset position, Δx is relabeled x_1 , making x_2 the velocity, and its derivative acceleration. In this case, M is the mass of the moving piece, or platen (not the magnetization density of the magnet), and F_d accounts for any additional disturbance force in the transverse direction. The constants c_1 through c_4 are used to help simplify the collection of geometric and material constants.

It is instructive to take the transfer function from the incremental current to the incremental displacement, ignoring for now any disturbance, and setting certain terms to zero (centered, with no bias current). This yields,

$$\frac{\mathbf{X}(s)}{\mathbf{I}(s)} = \frac{-D_i}{s^2 - D_x} \quad (8)$$

resulting in two poles (one of which is unstable) at the positions,

$$\omega_k = \sqrt{D_x} = \frac{1}{c_3} \sqrt{\frac{c_1 c_2}{m}} = \frac{M_0 l n}{h + l + n g} \sqrt{\frac{2 \mu_0 d t}{m g}} \quad (9)$$

As a brief note, it should be stated that linearization for the electrodynamic forces is trivial. When linearized, the centered result appears as the non-linearized form with Δx approaching zero.

Control systems are found in a variety of applications in the MOB design. Digital implementations of control loops are used to control the transverse motion of the platen as well its scanning motion. The control of the first of these two motions is particularly challenging, since the system is open-loop unstable in this axis

An unstable pole is commonly present in hybrid magnetic bearing systems. Many non-hybrid magnetic bearing systems of a similar nature to the one described herein utilize a lead compensator in one form or another to insure stabilization [4,5,6]. It will be shown in the subsequent section how such a lead compensator was applied to the transverse control. Such a controller is also well suited to the scanning motion.

The objectives of the control system may be summarized as follows. First and foremost in importance is achieving robust stabilization. Secondly, zero steady state error is important. If the mirror relies on the bearings to make corrections, then over some time the bearing must meet the exact corrections specified. Third, a fast settling time is desirable. The quicker corrections can be made, the better the system will be able to follow the command signals. Fourth, good disturbance rejection is desirable, to insure a isolation from external jitter. The quantitative design objectives are crossover at 200 Hz for the transverse motion, and 50 Hz for the scanning motion. The former number is based on the location of the unstable pole in the first case. The latter is based on desired tracking bandwidth capability. With these basic specifications in mind, the control systems may now be developed.

Though many of the same principles and parameters can be seen in the electromagnetic versus electrodynamic control system behavior, each one must be developed separately. Because transverse suspension was obtained, as is necessary before scanning travel can be pursued, it will be presented and developed in full.

A lead compensator in the feedback path is the first control element added to stabilize the system. PI control is then added on later to fine tune the controller and to insure a zero steady state error and good disturbance rejection. The overall setup of this loop is shown in the block diagram below (figure 5).

For the electromagnetic coils, the 200 Hz crossover was chosen, and a maximum phase margin was desired of about 60° , which corresponds to an α of 15 [7]. This is all the information needed to specify the time constants of the lead compensator. Several projects using magnetic bearings have argued for placing the lead compensator in the feedback path rather than traditional placement in the forward one [4, 6]. In practice, this leads to a system with the same rise time, but reduced control effort and overshoot. The addition of a PI controller is desirable to insure zero steady state error and provide better low-frequency disturbance rejection. The specific values are chosen to yield a quick settling time without adding too much reduction of phase margin.

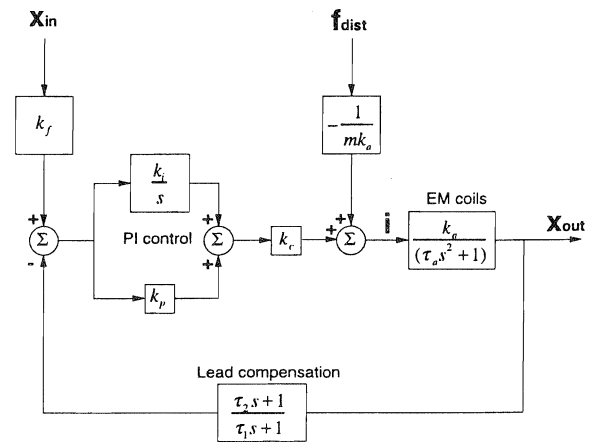


Figure 5: EM general block diagram.

5 Results

The goal was to use the lead compensator set at the 200 Hz crossover mark and see if the system could be controlled as predicted. The proportional gain as well as the compensator could both be attenuated for a stable system first without the integrator. When initial test were performed, it was shown that the theoretical value for the gain of the electromagnetic transfer function underestimated the actual value. This was most likely due to the three-dimensional effects of the magnets, since more of the permanent magnet flux comes into the e-cores from the permanent magnets on the sides, increasing the resultant MMF and hence, gain. Once a reasonable model of the plant was obtained, then fine adjustments of the control values based on the model could be made.

The testing procedure here is relatively straightforward; adjust the gain to attempt to get the system critically damped, then add the integrator. Once a reasonably good model of the plant was established by just lead and proportional control, good simulations of the system behavior could be performed with the modeling program Simulink. The model actually provided an excellent initial reference point in which to set the integrator gain to. Once incorporated, the integrator value could be modified, as well as the gain, for optimal response. There are two reasons for the addition of the integrator; to increase disturbance rejection, and, in this particular case, to decrease the rise time. Several different magnitudes of step responses were attempted with the controller with the results shown in figure 6. The range is from 1 micrometer, which borders the resolution capacity of the probe, to 15 micrometers.

Some brief comments on the post-step rippling are warranted here. The rippling throughout the entire system occurs at roughly 200 Hz. It is believed that this is due to a structural resonance associated with the pendulum structure which supports the testbed.

Once the voice coils are inserted, they can be immediately tested without the use of the digital control loop by means of a sinusoidal voltage signal generator. Using the mass-and-spring analogy, the scan direction can be driven at its natural frequency of about 2 Hz which happens to close to the scan rate specified in the overall system

requirements. In figure 7, the resultant scan motion when this loop is driven by a 50 mV sinusoid is shown.

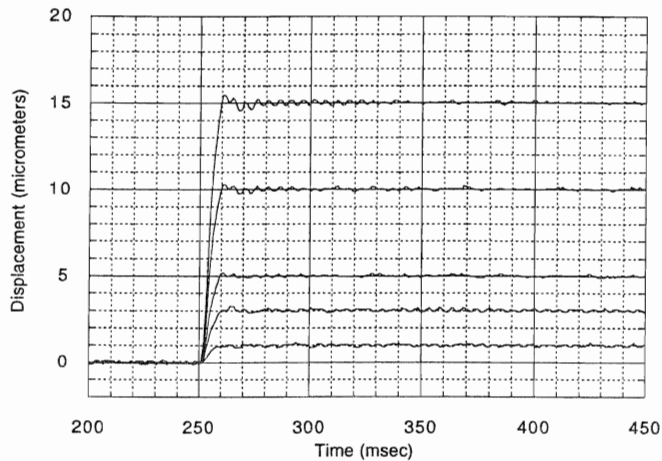


Figure 6: Positive step response of PI controlled system (displacement)

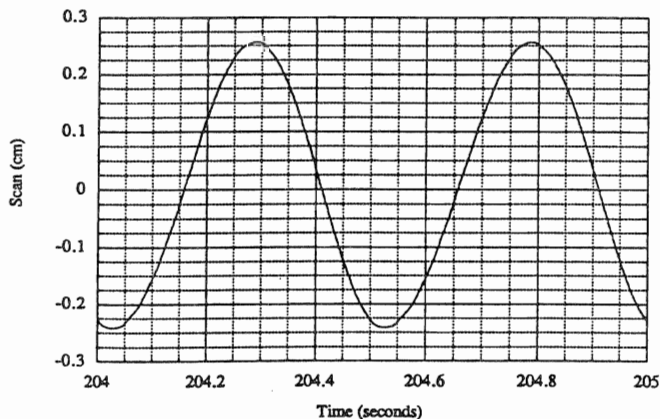


Figure 7: Open loop scanning oscillation.

7 Conclusion

The results of the study and the prototype offer some very promising possibilities for the future of the MOB design. The tests performed proved the hybrid capability of this unique magnetic circuit design. The concept may easily be transformed to a much smaller size.

In conclusion, the design is successful and opens the door to further exploration of the MOB hybrid magnetic bearing concept. With the technology base in place, the foundation for the full six degree-of-freedom scanning mirror has been established.

Scanning mirrors for interferometers are but one use for such a configuration as M.O.B. design and architecture. The interferometer is the most obvious case where a need arises for a system that has fairly large scanning capabilities and tight requirements on all other axes motion and angular displacements. This device may also be possibly used in such devices as coordinate measuring machines, linear axis control, lithographic steppers, and other precision control devices.

References

- [1] Johnston, S.F., *Fourier Transform Infrared: A Constantly Evolving Technology*. Ellis Horwood Limited, Chichester, England, 1991.
- [2] Akiba, T., Shingu, S., Kameda, Y., Akabane, S., and Hirai, S., "Development of a Magnetically-Suspended Mirror Scanning Mechanism for an Interferometer Monitor for Greenhouse Gases (IMG)," Third Int'l Symposium on Magnetic Bearings, Alexandria, VA, July 29-31, 1992.
- [3] Schwartz, L., "Magnetic Optical Bearing (MOB) Design for Mirror Wavelength Scans in a Spaceborne Interferometer," M.S. Thesis, M.I.T., Camb., Mass., 1995.
- [4] Trumper, D., "Magnetic Suspension Techniques for Precision Motion Control," Ph.D. Thesis, M.I.T., Camb., Mass., 1990.
- [5] Roberge, J.R., *Operational Amplifiers: Theory and Practice*. John Wiley & Sons, Inc., NY, New York, 1975. deVegte, J.V. (1990): *Feedback Control Systems*. Prentice-Hall, Inc., Englewood Cliffs, NJ, 1990.
- [6] Olson, S., "Nonlinear Compensation of a Single Degree of Freedom Magnetic Suspension System," M.S. Thesis, M.I.T., Camb., Mass., 1994.
- [7] deVegte, J.V., *Feedback Control Systems*. Prentice-Hall, Inc., Englewood Cliffs, NJ, 1990.